




Machine learning-based EEG signals classification model for epileptic seizure detection

Aayesha¹ · Muhammad Bilal Qureshi¹  · Muhammad Afzaal² ·
Muhammad Shuaib Qureshi³ · Muhammad Fayaz³

Received: 14 July 2020 / Revised: 8 October 2020 / Accepted: 25 January 2021 /
Published online: 12 February 2021

© The Author(s), under exclusive licence to Springer Science+Business Media, LLC part of Springer Nature 2021

Abstract

The detection of epileptic seizures by classifying electroencephalography (EEG) signals into ictal and interictal classes is a demanding challenge, because it identifies the seizure and seizure-free states of an epileptic patient. In previous works, several machine learning-based strategies were introduced to investigate and interpret EEG signals for the purpose of their accurate classification. However, non-linear and non-stationary characteristics of EEG signals make it complicated to get complete information about these dynamic biomedical signals. In order to address this issue, this paper focuses on extracting the most discriminating and distinguishing features of seizure EEG recordings to develop an approach that employs both fuzzy-based and traditional machine learning algorithms for epileptic seizure detection. The proposed framework classifies unknown EEG signal segments into ictal and interictal classes. The model is validated using empirical evaluation on two benchmark datasets, namely the Bonn and Children's Hospital of Boston-Massachusetts Institute of Technology (CHB-MIT) datasets. The obtained results show that in both cases, K-Nearest Neighbor (KNN) and Fuzzy Rough Nearest Neighbor (FRNN) give the highest classification accuracy scores, with improved sensitivity and specificity percentages.

Keywords Machine learning · Epilepsy · Seizure detection · Signal processing · EEG · Classification

1 Introduction

Epilepsy is a serious and the second most commonly occurring neurological disorder [45]. Over 65 million people across the world are suffering from this mental disorder, and every 26th individual is an epileptic patient [2]. Studies show that this disease is caused by the hyper-synchronous and excessive abnormal electrical activities of neuron cells, which impair both the

✉ Muhammad Bilal Qureshi
muhdbilal.qureshi@gmail.com

mental and physical health of the patient. A very common symptom of epilepsy is epileptic seizures that are highly unprovoked in nature [23]. To detect the occurrence of such seizures, neurologists recommend Electroencephalography (EEG) of the brain. It is a clinical-based test that captures the electrical activities of neurons and presents them as EEG records [34]. These recordings are complicated biomedical signals and difficult to investigate manually [41]. The major issue with manual inspection of EEG signals is the continuous availability of a neurologist, which is not possible in the case of long-term EEG recordings [40]. Furthermore, it is a tedious and time-consuming task that requires expert knowledge to accurately identify seizures [20]. To overcome these issues, the investigation of EEG signals is made automatic by employing machine learning algorithms. In this automation, characterizing features of EEG signals are extracted to train machine learning algorithms [21]. The trained algorithms build classifying models that perform the classification of EEG signals for the automatic detection of epileptic seizures.

The available approaches of automatic epileptic seizure detection encounter some challenges that lead to the inaccurate classification of EEG signals. One major challenge is the extraction of the most representative and distinguishing features of epileptic EEG signals. To focus on this challenge, it is necessary to tackle the nonlinear and non-stationary nature of EEG signals [12]. Since the dynamic nature of EEG signals causes variations in the characteristics of seizure recordings acquired from different seizure events, there are complications in extracting the most discriminating feature set of epileptic EEG signals. The second challenge is to reduce the misclassification rate, which is due to the fact that some of the oscillatory and fractal characteristics of seizure and seizure-free EEG signals resemble each other.

In order to address the aforementioned challenges, a framework for automatic epileptic seizure detection is proposed in this paper. This framework introduces a feature extraction method that gets temporal and spectral features from the decomposed signal sub-bands to obtain the time-domain and frequency-domain information about the morphological structure of EEG signals. Furthermore, to improve the accurate detection of epileptic seizures, fuzzy-based and traditional machine learning algorithms are employed for the classification of EEG signals. A comparative analysis with state-of-the-art works proves the effectiveness of the proposed methodology.

Research Contributions

The main contributions of this paper are stated as follows.

- An improved machine learning-based epileptic seizure detection model is proposed that categorizes EEG signals into ictal and interictal classes with an enhanced accuracy percentage.
- A feature extraction method is introduced that extracts the most distinguishing features of ictal EEG signals by employing a time and frequency-based statistical analysis of decomposed EEG signals.
- The optimal window size is empirically determined to split the EEG signal into segments for better interpretation of long-term EEG recordings.
- The performance comparison of traditional and fuzzy classifiers is conducted in terms of multiple metrics using single-channel and multi-channel benchmark EEG datasets.

The rest of the paper is organized as follows. Section 2 critically analyzes related literature works. Section 3 comprehensively explains the proposed model of machine learning-based

EEG signal classification for epileptic seizure detection. Section 4 discusses and comparatively analyzes the experimental results obtained using two different types of machine learning algorithms. Section 5 is dedicated to empirically analyzing the strategies incorporated into the proposed model and performing a comparison with state-of-the-art existing works. The last section presents the conclusion in terms of contributions and findings.

2 Previous approaches for epileptic seizure detection

This section discusses previously proposed machine learning-based approaches for epileptic seizure detection. The rationale is to critically analyze and find the limitations of the existing proposed works. The current methods use different signal processing techniques to extract useful features for classifying EEG signal recordings. However, the complicated nature of EEG signals is a barrier to distinguishing between seizure and non-seizure EEG recordings. Table 1 describes some acronyms used in this paper.

According to wavelet transform based-methods [2, 5, 12, 20, 21, 23, 27, 29, 34, 39, 40, 43], EEG signals are decomposed into sub-bands of varying frequency ranges. The characterizing features of decomposed signal sub-bands are extracted and input to machine learning algorithms that build models for classifying EEG signals into normal, ictal, and interictal classes.

In previous works [2], extracted Hilbert Envelopes of decomposed signals along with other features were used for building a classification model. This work showed 99.7% accuracy with KNN but was not applicable in clinical practices because it was not validated on various patient demographics. M. Mursalin et al. [23] proposed an ICFS technique that presented 98.45% accuracy with RF but could not accurately classify the EEG signals with high intra-class and low inter-class variability of feature values. In the same context, A. Subasi et al. [34] introduced the hybrid classifiers GA-SVM and PSO-SVM, which chose appropriate parameters of the SVM kernel function by optimizing algorithms. These classifiers provided results with a better accuracy of 99.38% but added the cost of high execution time. Y. Wang et al. [40] applied a three-level decomposition of LDWT along with a SELM classifier for EEG classification into normal, interictal, and ictal classes. It achieved 98.40% accuracy, but showed the quadratic programming problem while training its classifier.

In conformity with other epileptic seizure detection methods, M. Li et al. [20] proposed an NNE that built the model using the features obtained by DWT and presented a 98.78% classification accuracy. The same authors improved this performance in another study [21] to 98.87% by employing DT-CWT along with SVM. However, the high computational complexity, due to the building of an ensemble classifier and the implementation of DT-CWT, is a major drawback of these methodologies. Furthermore, several previous approaches failed to provide a pre-processing step before signal analysis [2, 20, 23, 34].

To classify EEG signals into interictal and ictal classes, Y. Gu et al. [12] first applied BSSCCA and ICA to remove EMG and EOG artifacts, respectively. Afterwards, the extracted temporal features built an SVM classification model that showed high false detection rates for clinical EEG and a low sensitivity of 94.5% for behind the ear EEG. For the same classification case, Orosco et al. [27] performed SWT and extracted statistical features to build models for LDA and BRNN. This work obtained a classification accuracy of 96.30% for the benchmark CHB-MIT dataset but did not provide a well generalized approach. Similarly, S. Patidar and T. Panigrahi [29] employed TQWT to extract Kraskov entropy from signal sub-bands. The entropy features built a classifying model of LS-SVM that correctly classified 97.7% of EEG recordings from the Bonn dataset.

Table 1 Descriptions of Acronyms

Acronym	Description
BRNN	Bayesian Regulation Neural Network
BSSCCA	Blind Source Separation of Canonical Correlation Analysis
CHB-MIT	Children's Hospital of Boston-Massachusetts Institute of Technology
DCNN	Deep Convolutional Neural Network
DT-CWT	Dual Tree - Complex Wavelet Transform
DWT	Discrete Wavelet Transform
ECT	Enhanced Curvelet Transform
EMG	Electromyogram
EOG	Electrooculogram
EWT	Empirical Wavelet Transform
FBSE	Fourier-Bessel Series Expansion
FD	Fractal Dimension
GA-SVM	Genetic Algorithm - Support Vector Machine
GLCM	Gray Level Co-occurrence Matrix
HWPT	Harmonic Wavelet Packet Transform
ICA	Independent Component Analysis
ICFS	Improved Correlation-based Feature Selection
LDA	Linear Discriminant Analysis
LDWT	Lifting-based Discrete Wavelet Transform
LS-SVM	Least Squares - Support Vector Machine
MEMD	Multivariate Empirical Mode Decomposition
MGT	Modified Graph Theory
NNE	Neural Network Ensemble
NPT	Novel Pattern Transformation
P-1D-CNN	Pyramidal One-Dimensional Convolutional Neural Network
PSO-SVM	Particle Swarm Optimization - Support Vector Machine
RBF	Radial Basis Function
RF	Random Forest
ROC	Receiver Operating Characteristics
RVM	Relevance Vector Machine
SVM	Support Vector Machine
SELM	Sparse Extreme Learning Machine
SWT	Stationary Wavelet Transform
TQWT	Tunable-Q Wavelet Transform
WELM	Weighted Extreme Learning Machine
WMRPE	Weighted Multiscale Renyi Permutation Entropy
WPT	Wavelet Packet Transform

However, no selection criteria were given to choose the RBF kernel function for the SVM classifier. In [5], A. Bhattacharyya and R. B. Pachori proposed a framework that built an RF-based classification model using the features of EWT decomposed EEG signals. It presented a 99.41% classification accuracy for long EEG recordings of the CHB-MIT dataset, but performance declined due to the use of small segments of EEG signals.

Q. Yuan [43] employed WPT to extract spectral and non-linear features of the Freiburg EEG dataset. The extracted features built the classification model of WELM. However, the complete information of epileptic EEG recordings could not be extracted due to the lack of temporal feature availability. L. S. Vidyaratne and K. M. Iftikharuddin [39] extracted HWPT decomposed EEG signals and non-linear features to build a classification model of RVM. This technique showed over-specificity and generated a high false alarm rate of seizure detection due to fewer seizure EEG recordings as compared to non-seizure recordings. In other words, performance results provided low sensitivity percentages. D. K. Atal and M. Singh [4]

proposed a methodology in which, first EEG data was pre-processed by ECT, and then MGT, NPT, FD, and GLCM techniques were employed to extract features. The extracted features built a novel RF classifier to perform classification and then identification of epileptic EEG signals. The evaluation of the proposed method was performed by four two-class cases of the Bonn dataset as well as class-wise empirical analysis, but was not evaluated on data from patients of a wide variety of demographics.

C. Mahjoub et al. [22] proposed a method in which three strategies were inspected for accurate EEG signal classification. In the first strategy, linear and non-linear features were extracted from raw data and after performing recursive feature elimination, the selected features were supplied to SVM for signal classification. In the second strategy, TQWT was performed before feature extraction, while in the third strategy, features were extracted from MEMD signal sub-bands. However, spectral features, which have prime importance in EEG signal classification, were not considered. V. Gupta and R. B. Pachori [13] proposed a novel method that considered the non-stationary characteristics of EEG signals. In this method, an FBSE technique was employed to collect EEG rhythms from which WMRPE features were extracted. The most important features were selected after ranking them using the Bhattacharyya space algorithm, entropy, ROC, Student's *t* test, and Wilcoxon methods. The selected feature vector built classifying models in RF, LS-SVM, and regression algorithms for epileptic seizure detection. However, no feature in this work identified the pattern trends of EEG signals to get information about structural variations.

I. Ullah et al. [37] proposed an ensemble deep learning model-based system for the classification of EEG signals. It consisted of three modules in which first, a preprocessing module normalized the input EEG recordings. In the second module, an augmentation scheme was applied on the preprocessed EEG signals, which were then delivered to an ensemble of P-1D-CNN. The third module fused the outputs of all P-1D-CNN models to get a final decision about epileptic seizure detection. This system was evaluated on the Bonn dataset, but the only weakness is the high storage requirement while deploying it in wearable devices. C. Park et al. [28] introduced a method by developing DCNN for the classification of multi-channel scalp EEG signals. In this method, features concerning the spatio-temporal correlation between EEG channels were extracted using two different types of convolutional layers in the deep classifying model. The first layer was a 1D convolutional layer that considered time-domain changes in ictal EEG recordings, and the 2D convolutional layer worked on spatial relationships between EEG channels. This model was evaluated with different sized EEG segments, but the maximum accuracy percentage could not exceed around 90%.

3 Proposed model

This paper proposes an improved model for the automatic detection of epileptic seizures, which classifies input EEG recordings into ictal and interictal classes to detect the seizure state of an epileptic patient, as shown in Fig. 1. It consists of six major steps: (1) EEG dataset collection, which describes the collected EEG signal recordings; (2) pre-processing, which removes artifacts from the input dataset; (3) signal splitting, which splits long EEG recordings into small epochs; (4) feature extraction, which extracts temporal and spectral features from decomposed signal sub-bands; (5) classifier building, which builds a classifier using traditional and fuzzy machine learning algorithms on the extracted feature vector; and (6) classifier evaluation, where the constructed classification models are evaluated using accuracy,

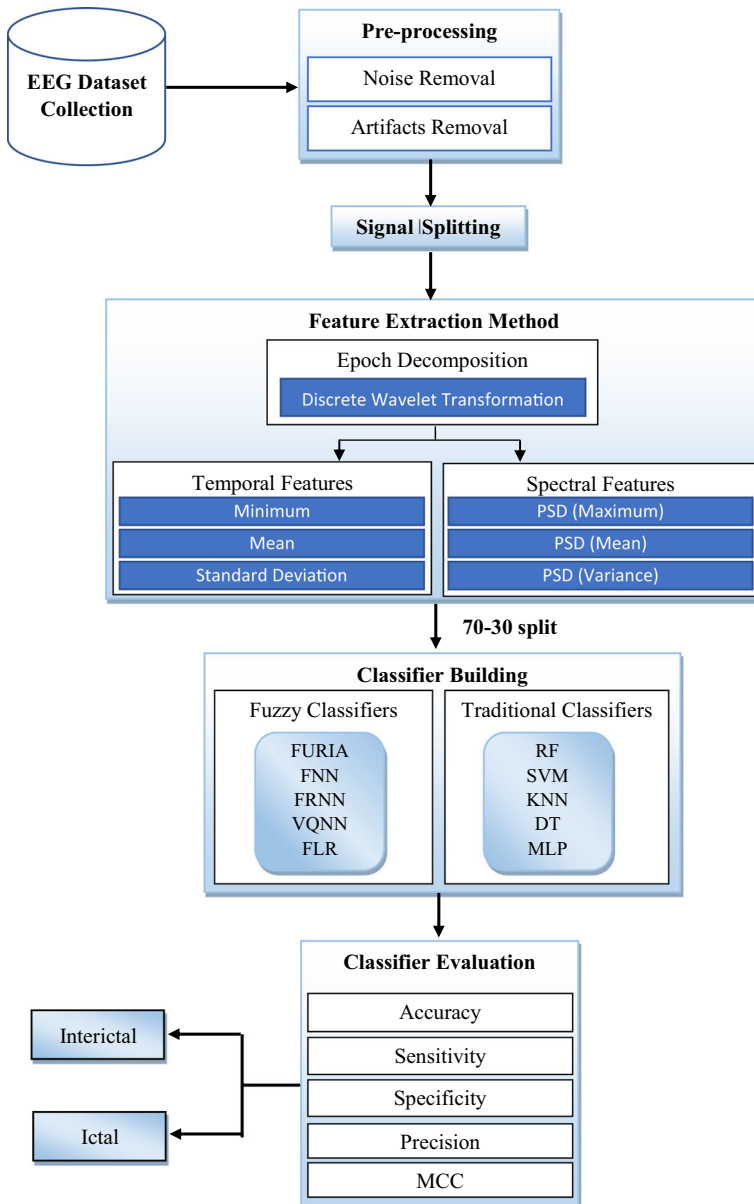


Fig. 1 Machine learning-based EEG signal classification model

sensitivity, specificity, precision, and the Matthews Correlation Coefficient (MCC). A detailed description of each step is provided in the following subsections.

3.1 EEG dataset collection

In the first step, two types of EEG signals are investigated: single-channel and multi-channel EEG recordings. These signals are acquired from two benchmark datasets, namely the Bonn

dataset and the CHB-MIT dataset. The Bonn dataset contains normal, interictal, and ictal EEG signals, whereas the CHB-MIT dataset is comprised of long interictal and ictal EEG recordings.

3.1.1 Bonn dataset

The Bonn dataset is a publicly available benchmark dataset that was collected by the Epileptology Department of Bonn University, Germany [1]. This dataset contains five subsets of single channel EEG signals: A, B, C, D, and E. Among these subsets, A and B consist of normal EEG signals, C and D are subsets of interictal EEG recordings, and E is comprised of ictal EEG recordings collected during the seizure states of the patient. These recordings have a sampling frequency of 173.61 Hz. In this dataset, one subset contains 100 signals of 23.6 s each that referred as 100×23.6 in the EEG recording column of Table 2. This table outlines a summary of only three subsets (C, D, E) from the Bonn dataset used in this study. It can be observed that the first column shows EEG Subset names, Health State demonstrates whether the patient is in a seizure or non-seizure state, Electrode Placement depicts the position of the EEG measuring electrodes on the scalp, and EEG Recording gives the lengths of EEG signals in seconds.

3.1.2 CHB-MIT dataset

Like the Bonn dataset, the CHB-MIT dataset is also a publicly available benchmark of EEG data acquired from the Children's Hospital Boston-Massachusetts Institute of Technology (CHB-MIT) [11]. It contains the EEG data of 24 patients with different demographics. This data consists of multi-channel scalp EEG recordings collected by employing the 10–20 system of electrode placement. It provides several hours of long interictal and ictal recordings of epileptic patients. The sampling frequency of this dataset is 256 Hz. Since the Bonn dataset was collected from five patients, in this paper only a small part of this entire dataset, consisting of five patients, is employed for inspection; the details are given in Table 3. According to this table, Patient ID, Gender, and Age show the personal details of the patient. The labels of Total EEG, Seizure (S) EEG, and Non-seizure (NS) EEG present the lengths of EEG recordings in seconds for the total, ictal, and interictal states of the patient, respectively.

3.2 Pre-processing

In the second step, the collected EEG signals are made noise-free by removing the artifacts that deteriorate the original recordings. Mostly, artifacts appear due to the movements of body limbs, or EMG, heart muscles, or ECG (Electrocardiogram), and eyes blinking, or EOG. These

Table 2 Outlines of the C, D, and E subsets of the Bonn dataset

EEG Subset	Health State	Electrode Placement	EEG Recording (seconds)
C	Interictal	Opposite to epileptogenic zone	100×23.6
D	Interictal	Within epileptogenic zone	100×23.6
E	Ictal	Within epileptogenic zone	100×23.6

Table 3 Description of the CHB-MIT dataset used

Patient ID	Gender	Age (year)	Total EEG (second)	Seizure EEG (second)	Non-seizure EEG (second)
P1	F	11	884	442	442
P2	M	11	344	172	172
P3	M	22	755	377	378
P4	F	1.5	306	153	153
P5	M	3	892	446	446

artifacts along with the environmental noise generated by electrode movement, embed in actual recordings that must be discarded. In the proposed methodology, the Butterworth filter [39] is applied to retain the signals in the desired frequency range and remove the noise-causing signals. This filter is configured to be a 0.5–60 Hz passband of 4th order, which allows only those frequency components of the signals that fall under the mentioned frequency range. It is mathematically defined as the following:

$$y(t)_{i-j} = BWF(x(t), i, j), \quad i = 0.5, \quad j = 60 \quad (1)$$

where *BWF* designates a Butterworth filter with an *i* to *j* frequency range applied on *x(t)* signals to obtain filtered *y(t)_{i-j}* EEG signals.

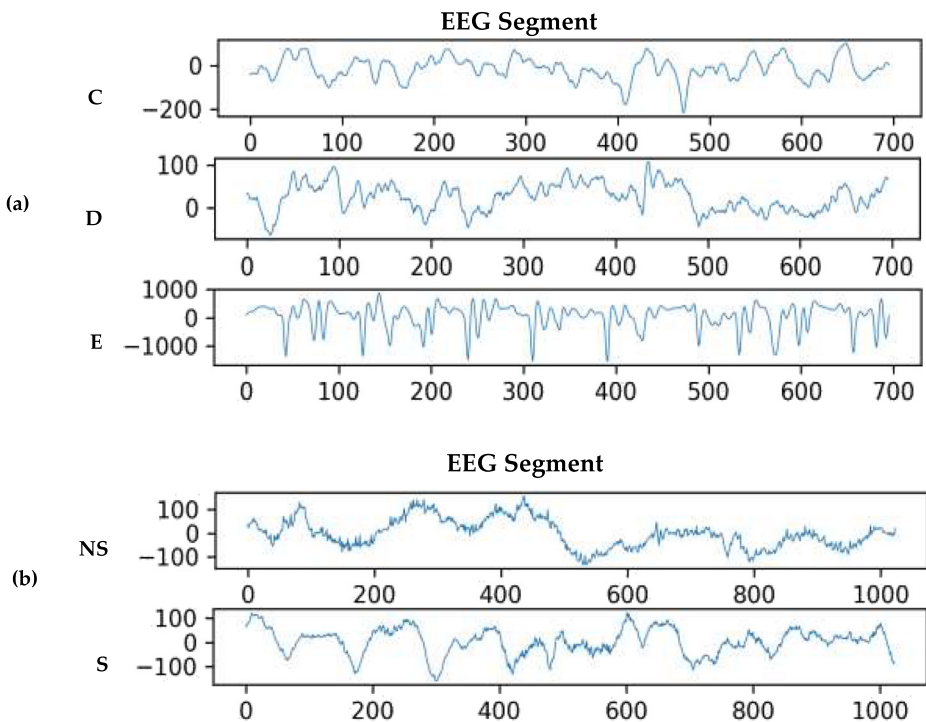


Fig. 2 **a** Segments of Bonn subset EEG recordings; **b** Segments of non-seizure and seizure CHB-MIT EEG recordings

3.3 Signal splitting

In the third step, the EEG signal time series are split into small segments or epochs so that they can be interpreted in a better way. This paper empirically evaluates different segment sizes of EEG signals in order to determine the appropriate size for epoch generations, as depicted in Algorithm 1. In this evaluation, segments of 1-s to 5-s are investigated with and without 50% overlap. It is observed that EEG epochs of 4-s with 50% overlap show the best performance in terms of classification accuracy, sensitivity, specificity, precision, and MCC metrics: therefore, this size is employed in the proposed method to generate small EEG epochs. Figures 2(a) and (b) show EEG segment instances from the Bonn and CHB-MIT datasets, respectively. In Fig. 2(a), C, D, and E refer to the epochs of Bonn data subsets, while NS and S in Fig. 2(b) represent the non-seizure and seizure EEG segments of the CHB-MIT data, respectively.

Algorithm 1. Pseudocode of Signal Splitting

1. **procedure**
 2. Take time series **t** of EEG signal recording; **i** = 0;
 3. Compute appropriate window size **ws** and window overlap **wo** for splitting of **t**;
 4. **while** termination condition is not satisfied **do**
 5. select window size **ws_i**; // in seconds
 6. select window overlap **wo_i**; // in percentage
 7. compute performance measures with **ws_i** and **wo_i**;
 8. **i** ++;
 9. **end while**
 10. return the best couple (**ws_i**, **wo_i**) to generate signal segments;
 11. **end procedure**
-

3.4 Feature extraction method

In this step, likewise [19, 24, 32] a feature extraction method is proposed that extracts the most distinguishing features from EEG signals to detect epileptic seizures. Algorithm 2 presents the pseudocode of the proposed method. It consists of two substeps: in the first substep, EEG epochs are decomposed into sub-bands by applying the DWT technique [33] of signal processing, which can be defined as the following:

$$\begin{aligned}
 &DWT(t, i, j) : \\
 &a_k, d_k = t(u, l), \quad \forall k \leq j \\
 &coeff \ni d_k, \quad \forall k \leq j \\
 &coeff \ni a_k, \quad k = j
 \end{aligned} \tag{2}$$

where the input EEG signal segment t is decomposed j times using the i wavelet function. For each decomposition, a pair of high-pass and low-pass filters (u , l) are applied to generate approximate (a_k) and detailed (d_k) sub-signals. It outputs a set of decomposed signal coefficients *coeff*.

In this paper, signal decomposition by DWT utilizes Daubachies 4 (db4) as the wavelet function, along with four levels of decomposition. In each decomposition level, the filter pair passes the signal components that fall in the frequency range defined by the filter pair. The four-level decomposition outputs five signal coefficients, including four detailed coefficients from d1 to d4 and one approximate coefficient a4. Each signal coefficient designates a certain frequency range, such as d1 (60–30 Hz), d2 (30–15 Hz), d3 (15–8 Hz), d4 (8–4 Hz), and a4 (4–0.5 Hz). Figures 3(a) and (b) represent the decomposed signal coefficients of the Bonn and CHB-MIT datasets, respectively.

The second substep of the feature extraction method allows the extraction of useful and discriminating statistical features from decomposed signal sub-bands. Two types of features, namely temporal and spectral, are extracted from each signal sub-band; overall, there are 30 features output from each EEG epoch.

The temple features represent the variety of EEG signals in the time domain. According to the proposed strategy, the minimum amplitude, mean amplitude, and standard deviation are extracted from each sub-band. Ref. [14] gives a mathematical formulation of temporal features as follows.

$$S_{min} = \min(sig) \quad (3)$$

$$\bar{S} = \sum_{k=1}^m \frac{sig_k}{m} \quad (4)$$

$$\sigma = \sqrt{\sum_{k=1}^m \frac{(sig_k - \bar{S})^2}{m}} \quad (5)$$

where S_{min} , \bar{S} , and σ designate the minimum, mean, and standard deviation of the amplitude for EEG signal signs of length m .

Since frequency is a fundamental characteristic of signals, frequency-based features of signals are extremely significant in capturing the non-stationary and non-linear properties of EEG signals. In the proposed feature extraction method, the Power Spectral Density (PSD) [27, 43] is extracted in terms of the maximum PSD [44], mean PSD [30], and variance of the PSD [30]. Mathematically,

$$P_{max} = \max(P(\omega)) \quad (6)$$

$$\bar{P} = \frac{\sum_{\omega} \omega P(\omega)}{\sum_{\omega} P(\omega)} \quad (7)$$

$$\sigma_S^2 = \frac{\sum_{\omega} (\omega - \bar{P})^2 P(\omega)}{\sum_{\omega} P(\omega)} \quad (8)$$

where $P(\omega)$, P_{max} , \bar{P} , and σ_S^2 indicate the power of a certain frequency, the signal frequency for which power is maximum, the value of the frequency at which the signal power spectrum is centered, and variations in power for different frequencies in a signal, respectively.

Algorithm 2. Pseudocode of Feature Extraction Method

```

1.  procedure
2.      Take a set of  $n$  EEG signal epochs;  $i = 0$ ;
3.      Extract a multi – dimensional feature vector  $\mathbf{FV}$ ;
4.      while termination condition is not satisfied do
5.          apply Discrete wavelet transformation; //get decomposed signal sub-bands
6.          for each decomposed signal of EEG do
7.              perform time – domain analysis; //extract temporal features
8.              perform frequency – domain analysis; //extract spectral features
9.          end for
10.         performance – based comparative analysis of extracted features;
11.          $i++$ ;
12.     end while
13.     return the most discriminating feature vector  $\mathbf{FV}$  from EEG signals;
14. end procedure

```

3.5 Classifier building

In the fifth step, the extracted features are used to train algorithms that build classification models. In this paper, five traditional machine learning algorithms, K-Nearest Neighbor (KNN), Decision Tree (DT), Random Forest (RF), Support Vector Machine (SVM), and Multilayer perceptron (MLP), and five fuzzy machine learning algorithms, Fuzzy Unordered Rule Induction Algorithm (FURIA), Fuzzy Nearest Neighbor (FNN), Fuzzy Rough Nearest Neighbor (FRNN), Vaguely Quantified Nearest Neighbor (VQNN), and Fuzzy Lattice Reasoning (FLR), are applied to build models for EEG signal classification.

3.5.1 Traditional machine learning algorithms

KNN is the simplest supervised machine learning tool for classification [14]. It is dependent on the number of predefined nearest neighbors, or the value of K . To classify the test object, the Euclidean distance between neighboring objects is measured and then the majority class among K neighbors is assigned to the test object. Furthermore, for feature selection, it takes advantage of data instances correlation.

DT predicts the correct class by dividing the instance space recursively [14]. It consists of multiple nodes of two types: leaf nodes and decision nodes. Like a tree, each decision tree starts with the root node and continues with several repetitive partitions before ending at leaf nodes. In the current study, J48 is employed as a DT machine learning algorithm for classification.

RF is an ensemble machine learning algorithm that is employed to perform classification and regression tasks [8]. As the name indicates, it is comprised of a number of decision trees. The output of RF is a combined output of multiple decision trees, where each tree predicts the

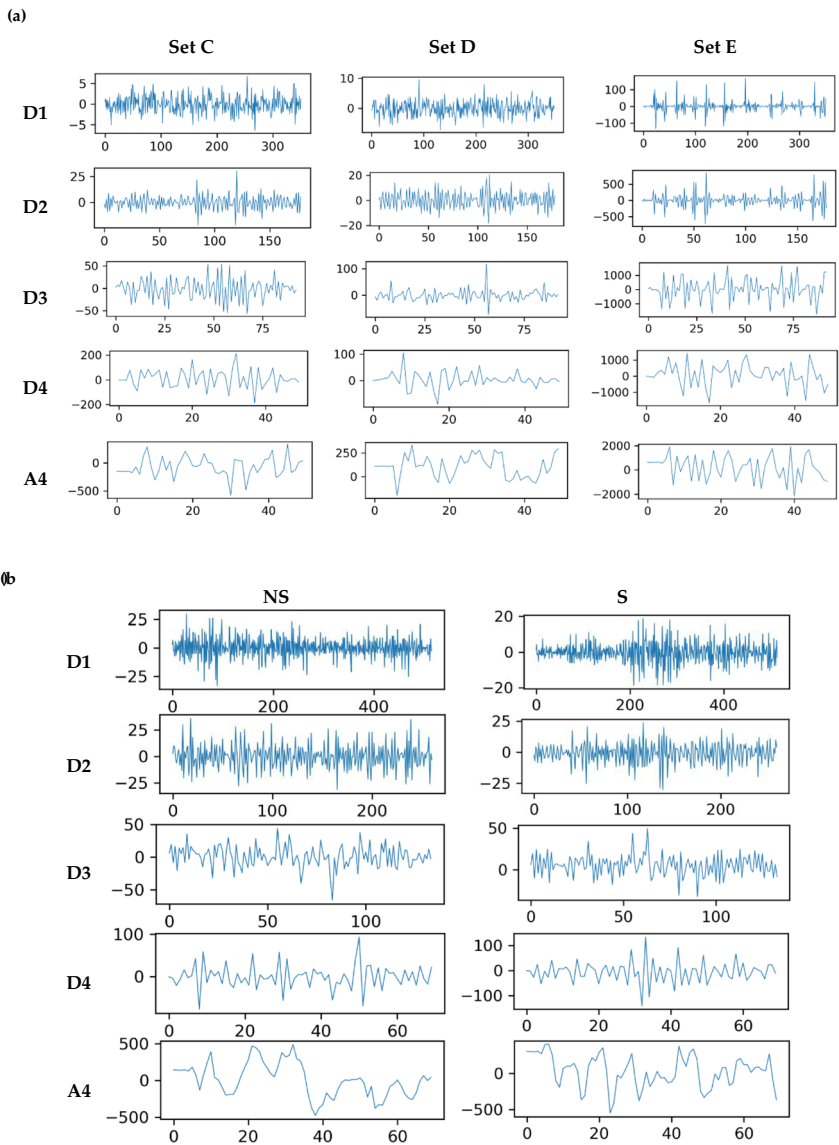


Fig. 3 **a** Decomposed sub-bands of the Bonn dataset. **b** Decomposed sub-bands of the CHB-MIT recordings

appropriate class based on the independent but identically distributed sample of random vector values. One of the major advantages of RF is its robustness towards noise.

SVM is a state-of-the-art algorithm that is mostly employed for pattern recognition and feature reduction [38]. It draws a hyperplane for the classification of instances into their corresponding classes. The margin between the hyperplane and boundary aligned support vectors for each class is maximized. It applies the linear discriminant function for binary classification; however, for non-linearly separable data, the RBF kernel is adopted.

MLP is an Artificial Neural Network (ANN) [26]. In general, ANNs try to mimic the brain's structure. An ANN is a network of neurons or nodes that are connected by different

Table 4 Partition of data into training and testing subsets

Dataset	Classification case	Training subset (No. of EEG epochs)	Testing subset (No. of EEG epochs)
Bonn EEG	C-E	1260	540
	D-E	1260	540
	CD-E	1890	810
CHB-MIT EEG	NS-S	1102 × 23	472 × 23

weights. MLPs have an input layer and one or more hidden layers with different numbers of nodes. The number of outputs is decided by the network type. In this study, we use two hidden layers, with half of the number input variables as hidden nodes.

3.5.2 Fuzzy machine learning algorithms

FURIA learns classification rules to employ a greedy approach by implementing a divide and conquer strategy [15]. The algorithm First-Order Inductive Learner (FOIL) is utilized to perform the rule growing that initiates with the shortest rule. The selection of features for rules is dependent on the measure of FOIL's Information Gain (IG). The highest value of IG designates an improved rule for a particular target class.

FNN performs classification based on the fuzzy similarity and membership degree computation [9]. This algorithm first determines the weighted distance between the *K* nearest neighbors and classifying objects. Afterward, the membership degree of neighboring objects for all the available classes is calculated to classify the test instance.

FRNN is a combination of FNN and fuzzy rough approximation [31]. It measures the similarity value between a test object and the neighboring training objects. The similarity value is used to measure the upper and lower approximations of the neighboring objects for each class. The obtained approximations are used to predict test object memberships for all classes. Eventually, the combination of upper and lower memberships assigns a class to the test object.

VQNN is a modified derivative of FRNN [17]. It employs VQRS approximation quantifiers such as “some” and “most” for lower and upper approximations, respectively. Since these approximations are less affected by noise, they are comparatively favorable. The test object classification is performed by utilizing the upper and lower approximations of the nearest neighbors for each class.

FLR infers rules from training data for the classification of testing instances [18]. Each fuzzy lattice is comprised of a lattice *L* and its valuation function *u*, which are indicated as a

Table 5 Performance results of C-E classification for traditional classifiers

Classifier	Accuracy (%)	Sensitivity (%)	Specificity (%)	Precision	MCC
RF	99.63	99.24	100	0.996	0.993
SVM	98.70	97.73	99.64	0.987	0.974
KNN	99.81	99.62	100	0.998	0.996
DT	99.44	99.24	99.64	0.994	0.989
MLP	99.07	98.11	100	0.991	0.982

Table 6 Performance results of C-E classification for fuzzy classifiers

Classifier	Accuracy (%)	Sensitivity (%)	Specificity (%)	Precision	MCC
FURIA	99.63	99.24	100	0.996	0.993
FLR	96.30	98.48	94.20	0.964	0.927
FRNN	99.81	99.62	100	0.998	0.996
VQNN	99.44	98.86	100	0.995	0.989
FNN	99.63	99.24	100	0.996	0.993

couple (L, u) . The induced fuzzy rules implement functions that consist of objects and their relative classes. On the basis of the inclusion measure, these rules compete for the classification of testing instances.

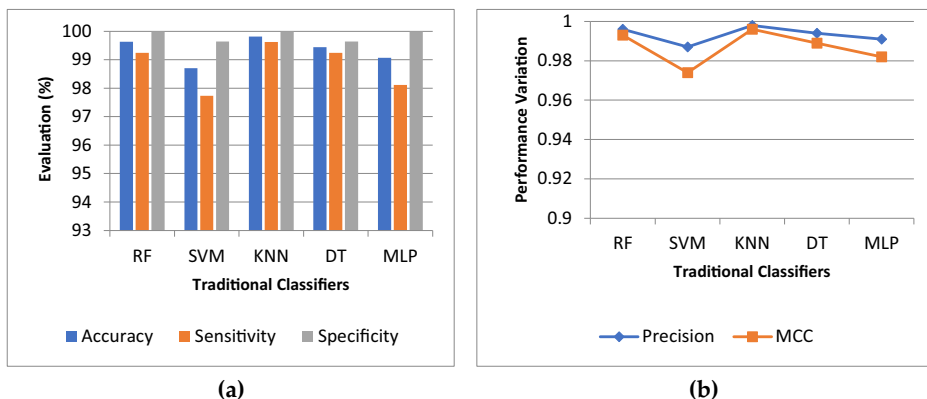
3.6 Classifier evaluation

In the last step, the constructed classification models are evaluated by testing EEG instances in terms of five performance measures, namely accuracy, sensitivity, specificity, precision, and MCC. Accuracy, as given in Eq. (9) [23], gives the percentage of total correctly classified EEG signal segments. Sensitivity and specificity measures indicate the percentages of correctly classified ictal and interictal signal segments, respectively, as referred to in Eqs. (10) [20] and (11) [29]. Precision represents the correctness of seizure or ictal detection results, as formulated in Eq. (12) [37]. The MCC evaluates the classifier's performance as a correlation coefficient, as shown in Eq. (13) [7].

$$\text{Accuracy} = \frac{TP + TN}{TP + TN + FP + FN} \times 100 \quad (9)$$

$$\text{Sensitivity} = \frac{TP}{TP + FN} \times 100 \quad (10)$$

$$\text{Specificity} = \frac{TN}{TN + FP} \times 100 \quad (11)$$

**Fig. 4** Comparison of traditional classifiers for C-E classification

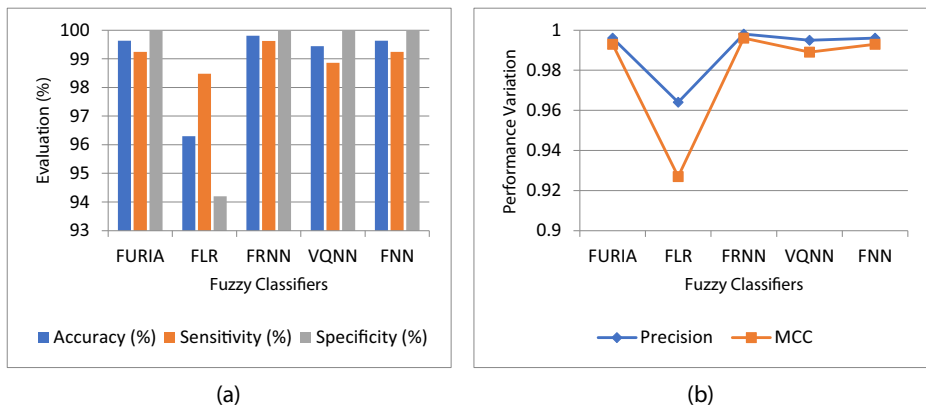


Fig. 5 Comparison of fuzzy classifiers for C-E classification

$$Precision = \frac{TP}{TP + FP} \times 100 \quad (12)$$

$$MCC = \frac{TP \times TN - FP \times FN}{\sqrt{(TP + FN)(TP + FP)(TN + FN)(TN + FP)}} \quad (13)$$

where TN, FP, TP, and FN represent True Negative, False Positive, True Positive, and False Negative, respectively. TN indicates the number of non-seizure EEG recordings accurately classified as non-seizure, while FP specifies the count of non-seizure signals falsely classified as seizures. On the other hand, TP designates the proportion of seizure instances correctly predicted to be seizures, and FN states the number of seizure recordings incorrectly predicted to be non-seizure signals.

4 Experiments and results discussion

In order to evaluate the proposed model, two sets of experiments were conducted using benchmark EEG datasets. In the first experimental set, the single-channel Bonn EEG dataset

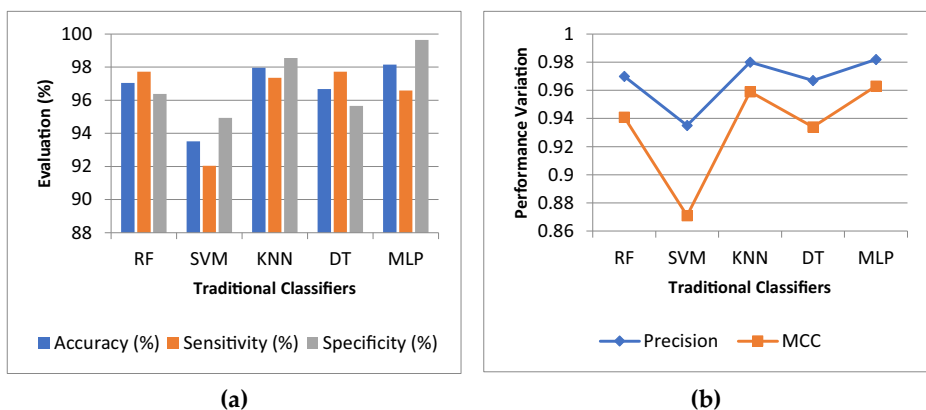


Fig. 6 Comparison of traditional classifiers for D-E classification

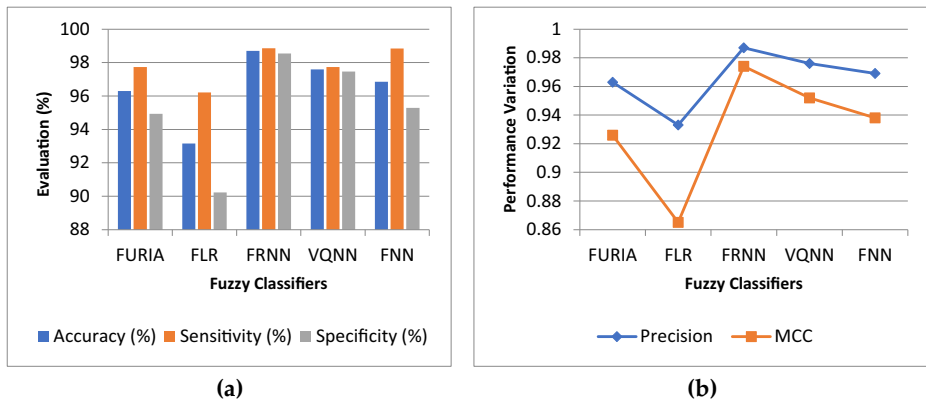


Fig. 7 Comparison of fuzzy classifiers for D-E classification

is used for evaluation, while in the second experimental set, the multi-channel CHB-MIT EEG dataset is utilized along with five traditional algorithms (RF, SVM, KNN, DT, MLP) and five fuzzy machine learning algorithms (FURIA, FNN, FRNN, VQNN, FLR).

For experimentation, the single channel Bonn dataset consists of a total of 2700 EEG epochs in which each subset (C, D, and E) contains 900 epochs. On the other hand, multi-channel CHB-MIT dataset has total 1574×23 (where 23 refers to number of channels) EEG epochs including 787×23 epochs of each subset (NS, S). In each classification case, dataset is partitioned into training and testing subsets by a 70/30 split of data. The training subset of 70% is used to build classifying models, and the testing subset of 30% is employed to evaluate the performance of classifiers. Table 4 presents the number of EEG segments that are used as training and testing instances for under investigation classification cases. The experiments were carried out using the Python and WEKA (Waikato Environment for Knowledge Analysis) classification toolbox on a multicore system with a 1.80 GHz processor. The results obtained are discussed in the following subsections.

4.1 Single-channel EEG recordings (Bonn dataset)

This section discusses an analysis of the results obtained by employing traditional and fuzzy classifiers using the single-channel EEG recordings of the Bonn dataset.

4.1.1 C-E classification case

The classification results achieved in the C-E classification case are given in Tables 5 and 6. The results show that KNN provided superior performance for the five performance metrics as

Table 7 Performance results of D-E classification for traditional classifiers

Classifier	Accuracy (%)	Sensitivity (%)	Specificity (%)	Precision	MCC
RF	97.04	97.73	96.38	0.970	0.941
SVM	93.52	92.04	94.93	0.935	0.871
KNN	97.96	97.35	98.55	0.980	0.959
DT	96.67	97.73	95.65	0.967	0.934
MLP	98.15	96.59	99.64	0.982	0.963

Table 8 Performance results of D-E classification for fuzzy classifiers

Classifier	Accuracy (%)	Sensitivity (%)	Specificity (%)	Precision	MCC
FURIA	96.30	97.73	94.93	0.963	0.926
FLR	93.15	96.21	90.22	0.933	0.865
FRNN	98.70	98.86	98.55	0.987	0.974
VQNN	97.59	97.73	97.46	0.976	0.952
FNN	96.85	98.84	95.29	0.969	0.938

compared to other traditional machine learning algorithms. The second-best classifier was RF, which showed 99.63% accuracy and 100% specificity. DT achieved 99.44% accuracy along with 0.994 precision, while MLP presented 99.07% correct EEG classification with 100% specificity. However, SVM showed the worst performance for all metrics except specificity. Table 6 demonstrates the fuzzy classifier results for the C-E classification case. In these results, FRNN showed the best performance, with 99.81% accuracy and 100% specificity. FURIA, FNN, and VQNN also achieved 100% specificity, but performance for other measures declined. FURIA and FNN showed equivalent accuracies of 99.63%, while that of VQNN was reduced to 99.44%. Poor results were obtained from FLR, which classified only 96.30% of EEG instances correctly. It is observed that KNN and FRNN obtained similar results for all performance metrics and showed the best performance as compared to other machine learning algorithms.

Figures 4(a) and (b) and 5(a) and (b) show the graphical representation of the comparison results for the C-E classification case by simulating traditional and fuzzy machine learning algorithms.

4.1.2 D-E classification case

For the D-E classification case, the traditional machine learning algorithm MLP exhibited the best performance, with 98.15% accuracy and 99.64% specificity, as plotted in Figs. 6(a) and (b). KNN proved to be the second-best classifier, with 97.96% accurate EEG signal classification. RF and DT provided comparable performance with the equivalent sensitivities of 97.73%. Figure 6(b) presents the measures of precision and MCC, where MLP attained the highest results of 0.982 and 0.963, respectively. In the case of the fuzzy classifiers, FRNN provided the maximum performance for all metrics, with 98.70% accuracy. Among other classifiers, VQNN achieved an accuracy of 97.59% and a specificity of 97.46%, but FNN yielded 96.85% accuracy with 98.84% sensitivity. Figures 7(a) and (b) plot the results for fuzzy classifiers using different performance measurement criteria. In the D-E classification case, the fuzzy classifier FRNN presented the highest performance among all traditional and

Table 9 Performance results of CD-E classification for traditional classifiers

Classifier	Accuracy (%)	Sensitivity (%)	Specificity (%)	Precision	MCC
RF	98.76	97.34	99.45	0.988	0.972
SVM	96.42	90.49	99.27	0.965	0.918
KNN	98.76	98.48	98.90	0.988	0.972
DT	96.91	96.20	97.26	0.969	0.930
MLP	98.89	98.10	99.27	0.989	0.975

Table 10 Performance results of CD-E classification for fuzzy classifiers

Classifier	Accuracy (%)	Sensitivity (%)	Specificity (%)	Precision	MCC
FURIA	98.15	97.34	98.53	0.982	0.958
FLR	93.70	99.62	90.86	0.947	0.871
FRNN	99.38	99.24	99.45	0.994	0.986
VQNN	99.14	99.24	99.09	0.991	0.980
FNN	98.64	98.86	98.54	0.987	0.969

fuzzy machine learning algorithms. The numerical statistics for both types of algorithms are given in Tables 7 and 8.

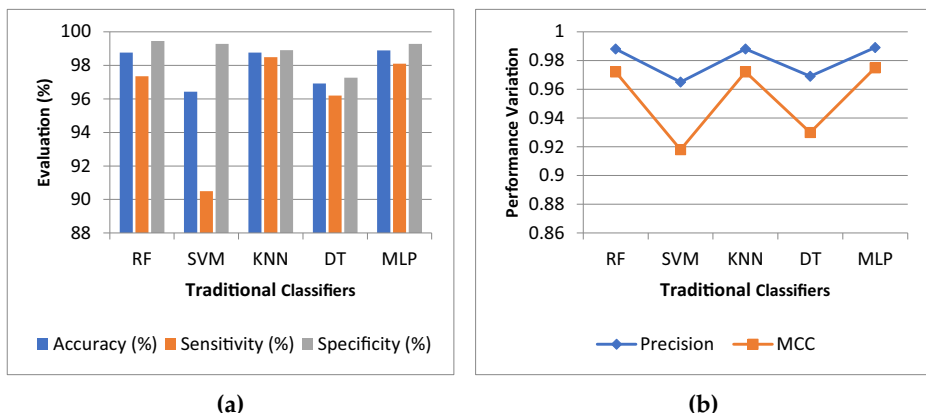
4.1.3 CD-E classification case

In regard to the experimental results on the CD-E classification case, Table 9 shows the performance values of traditional machine learning algorithms, while Table 10 gives the results of fuzzy classifiers for all metrics. To present a graphical demonstration, Fig. 8(a) depicts that MLP obtained the highest classification accuracy, precision, and MCC values of 98.89%, 0.989, and 0.975, respectively. The highest sensitivity of 98.48% was achieved by KNN, while the maximum specificity of 99.45% was provided by RF. In fuzzy classifiers, Fig. 9(a) illustrates the dominance of FRNN, with the highest accuracy and specificity measures of 99.38% and 99.45%, respectively. VQNN also revealed a comparable performance of 99.14%; however, for FNN and FURIA, the accurate EEG signal classification declined to 98.64% and 98.15%, respectively. In the case of FLR, the smallest accuracy of 93.70% and the highest sensitivity of 99.62% were achieved.

For precision and MCC measurements, the results of traditional and fuzzy classifiers are plotted in Figs. 8(b) and (b). The classifier with the highest percentage accuracy showed the best precision and MCC results.

4.2 Multi-channel EEG recordings (CHB-MIT dataset)

In this section, the classification results of traditional and fuzzy classifiers are analyzed using the multi-channel scalp EEG recordings of the CHB-MIT dataset.

**Fig. 8** Comparison of traditional classifiers for CD-E classification

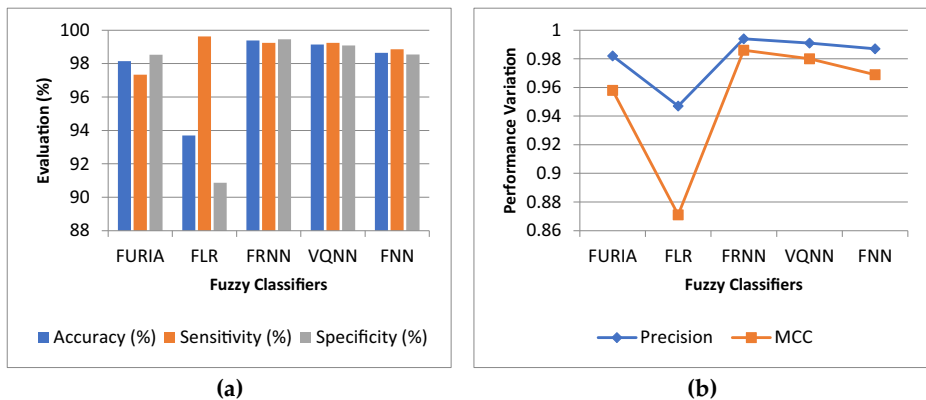


Fig. 9 Comparison of fuzzy classifiers for CD-E classification

4.2.1 NS-S classification case

The performance of traditional and fuzzy classifiers for the multi-channel NS-S classification case is provided in Tables 11 and 12. According to the reported results, Fig. 10(a) describes that KNN achieved the highest classification accuracy of 91.09%, while RF obtained the highest sensitivity percentage of 92.54%. The maximum specificity of 92.29% was provided by MLP, with reduced accuracy and sensitivity percentages of 85.71% and 78.99%, respectively. On the other hand, SVM could not show notable results for any performance metric. In fuzzy classifiers, Fig. 11(a) demonstrates that FRNN outperforms its counterparts with 92.76% accuracy and 93.62% specificity, as presented in Table 12. For VQNN, the obtained accuracy was 92.05% with 93.58% specificity. In the case of FNN and FURIA, the provided results were equivalent, with 90.21% classification accuracy. The smallest accuracy of 86.81% was achieved by FLR, with 91.54% sensitivity and the lowest specificity of 82.42%.

The performance measures precision and MCC were the highest for the KNN and FRNN classifiers in traditional and fuzzy classifiers, respectively, as shown graphically in Figs. 10(b) and 11(b).

5 Comparative analysis

This section discusses the comparison of classification results obtained from the Bonn and CHB-MIT EEG datasets. The performance of classifiers is analyzed for both

Table 11 Performance results of NS-S classification for traditional classifiers

Classifier	Accuracy (%)	Sensitivity (%)	Specificity (%)	Precision	MCC
RF	90.60	92.54	88.70	0.907	0.813
SVM	81.34	75.70	86.86	0.817	0.630
KNN	91.09	90.32	91.83	0.911	0.822
DT	87.60	88.07	87.13	0.876	0.752
MLP	85.71	78.99	92.29	0.863	0.720

Table 12 Performance results of NS-S classification for fuzzy classifiers

Classifier	Accuracy (%)	Sensitivity (%)	Specificity (%)	Precision	MCC
FURIA	90.21	89.32	91.09	0.902	0.804
FLR	86.81	91.54	82.42	0.862	0.767
FRNN	92.76	91.89	93.62	0.928	0.855
VQNN	92.05	90.49	93.58	0.921	0.841
FNN	90.21	89.32	91.09	0.902	0.804

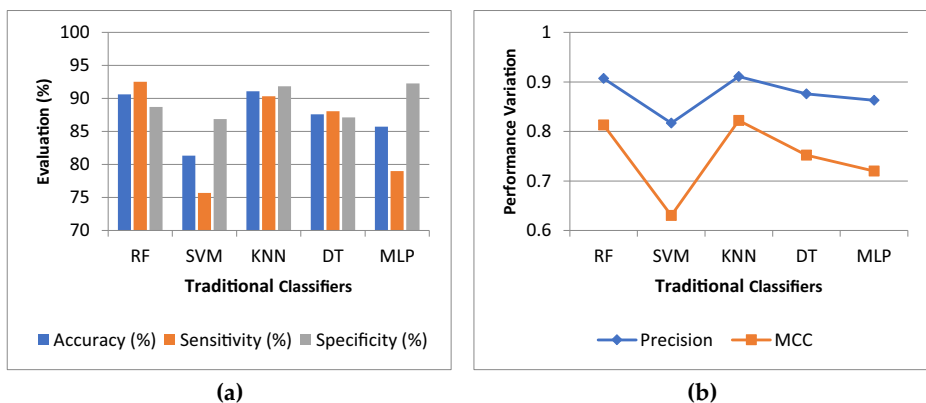
datasets. The comparative analysis of the proposed methodology is also conducted with the existing state-of-the-art methodologies for ictal versus interictal classification of EEG signals.

5.1 Performance comparison based on single and multi-channel EEG recordings

It is observed that in the case of EEG recordings from the Bonn dataset, the classification accuracies of KNN and MLP are the highest among traditional machine learning algorithms, as depicted in Fig. 12(a). On the other hand, Fig. 12(b) shows that, for fuzzy classifiers, FRNN gives the best accuracy as compared to the others. For the CHB-MIT dataset, KNN presents the best performance among traditional classifiers, while FRNN proves the best performance among fuzzy classifiers, as illustrated by Fig. 13(a) and (b).

5.2 Analysis of signal splitting strategy

In this section, an empirical analysis is conducted for different sizes of EEG segments. Table 13 provides the classification accuracy percentages of the CD-E and NS-S classification cases for different window sizes. The rationale of this analysis is to choose the length of an EEG segment that improves signal interpretation and as a result, enhances the classification accuracy. The obtained results show that a 4-s EEG segment with 50% overlap with the previous segment results in the highest performance. The graphical representation of classifier performance for different segment sizes is plotted in Fig. 14.

**Fig. 10** Comparison of traditional classifiers for NS-S classification

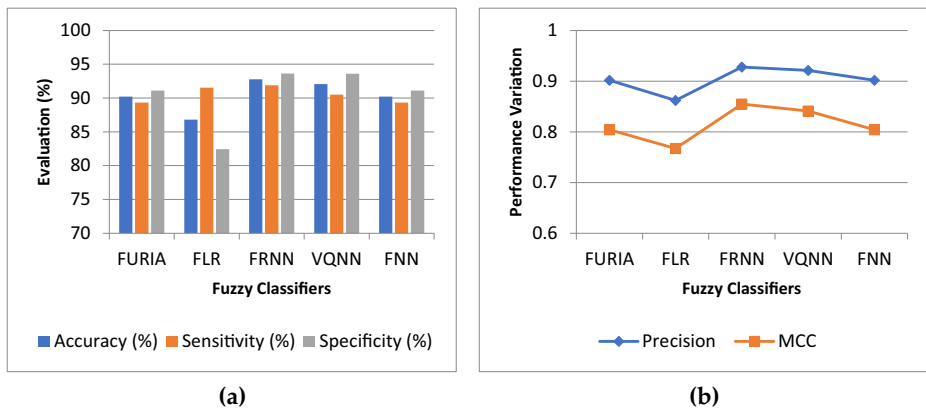


Fig. 11 Comparison of fuzzy classifiers for NS-S classification

It can be observed that for the CD-E classification of the Bonn dataset, accuracy slowly improves with increasing segment size and reaches its peak at the size of 4-s with 50% overlap. Similarly, in the case of the NS-S classification of the CHB-MIT dataset, performance gradually improves with increasing segment size, but the segments with 50% overlap showed better performance than the others without overlap.

5.3 Analysis of the feature extraction method

The feature extraction method is also empirically analyzed by conducting a comparison with different feature vectors. Table 14 presents the EEG classification accuracy score of FRNN for four classification cases using different feature vectors, and Fig. 15 graphically plots the performance comparison. In this comparison, the percentage accuracy provided by the proposed feature vector of temporal and spectral features is comparatively analyzed with those obtained from temporal and spectral features separately.

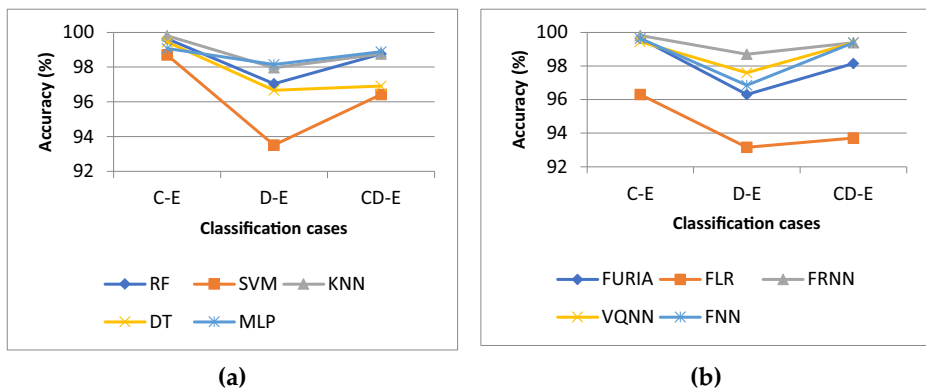


Fig. 12 **a** Comparison of traditional classifiers for the Bonn dataset; **b** Comparison of fuzzy classifiers for the Bonn dataset

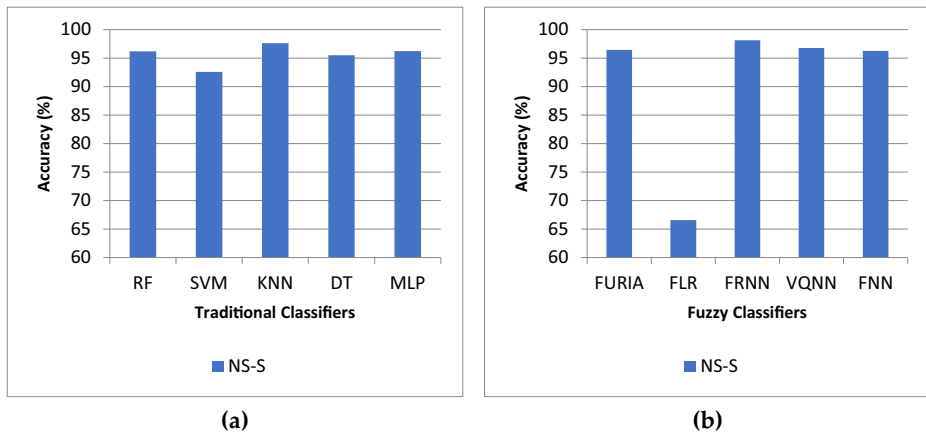


Fig. 13 **a** Comparison of traditional classifiers for the CHB-MIT dataset; **b** Comparison of fuzzy classifiers for the CHB-MIT dataset

An overview of the obtained results demonstrates the predominant performance of the proposed feature vector as compared to the temporal and spectral features of non-transformed EEG signals. In contrast, the temporal and spectral features of decomposed EEG signals on an individual basis provided notable improvements. However, the combined feature vector of decomposed EEG signals achieved the highest performance for all classification cases.

5.4 Comparative analysis of extracted features with existing EEG features

In this section, a comparison is performed between the proposed extracted feature vector and other existing EEG features as employed in [35, 46]. Table 15 represents the performance results of different types of features, including the approximate entropy [3], Hurst exponent [44], fractal dimension [21], and LBP features [36] that determine the randomness, non-linearity, complexity, and patterns of EEG signals. Although these features are extensively utilized in literature, the proposed feature vector of temporal and spectral features provided the best results by determining the morphology of dynamic EEG signals' time series. Figure 16

Table 13 Comparative analysis of different EEG signal segments

Segment size (second)	(Accuracy %)	
	CD-E	NS-S
1-s	97.39	83.59
1 s with 50% overlap	97.09	87.38
2-s	97.78	85.67
2 s with 50% overlap	98.36	90.19
3-s	97.94	86.98
3 s with 50% overlap	98.38	91.81
4-s	97.78	87.32
4 s with 50% overlap	99.44	92.76
5-s	99.44	88.08

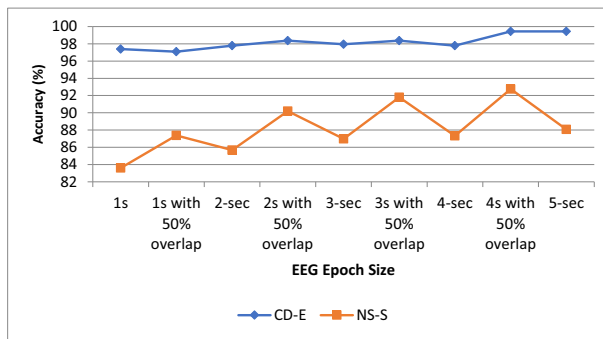


Fig. 14 The comparison of different signal segments for EEG classification

portrays the performance differences among different features for all of the classification cases of epileptic seizure detection under investigation. In this observation, the proposed feature vector is at the top, and the Hurst exponent provides the worst performance. On the other hand, the fractal dimension provides relatively impressive performance, but the entropy and LBP features could not attain significant classification accuracies.

5.5 An empirical analysis using deep learning and Hypergraph learning classifiers

This section is dedicated to conduct an empirical analysis with deep learning and hypergraph learning algorithms for EEG signal classification. In this paper, three deep learning algorithms, Deep Neural Network (DNN) [25], One-Dimensional-Convolutional Neural Network (1D-CNN) [16], and Long Short Term Memory (LSTM) [6], and two Hypergraph Learning algorithms; Hypergraph Neural Network (HGNN) [10] and Hypergraph Convolutional Network (HyperGCN) [42] are used to perform seizure versus non-seizure classification experiments with Bonn as well as the CHB-MIT EEG datasets. The evaluation results of the built classifiers are shown in Table 16. According to these results, DNN is dominant in C-E and D-E classification cases while LSTM proves the best for CD-E and NS-S classification cases.

By employing deep learning classifiers for C-E classification case, DNN provided the most remarkable performance with 99.81% accuracy and 99.62% sensitivity. The performance of LSTM and 1D-CNN was comparable with 98.89% and 98.22% accuracy respectively. The highest specificity of 100% achieved by DNN and LSTM. In D-E classification case, DNN performed impressively by achieving 97.96% accuracy and sensitivity percentage of 96.97% equivalent to LSTM. In this classification case, 1D-CNN provided slightly inferior accuracy of

Table 14 Performance results of different feature vectors for EEG classification

Classification case	Accuracy (%)				
	Temporal	Spectral	DWT+ Temporal	DWT+ Spectral	Proposed method (DWT + Temporal+Spectral)
C-E	98.70	96.67	99.81	99.07	99.81
D-E	95.56	91.11	98.52	97.78	98.70
CD-E	96.79	93.46	98.52	98.39	99.38
NS-S	73.48	73.55	92.76	86.92	92.79

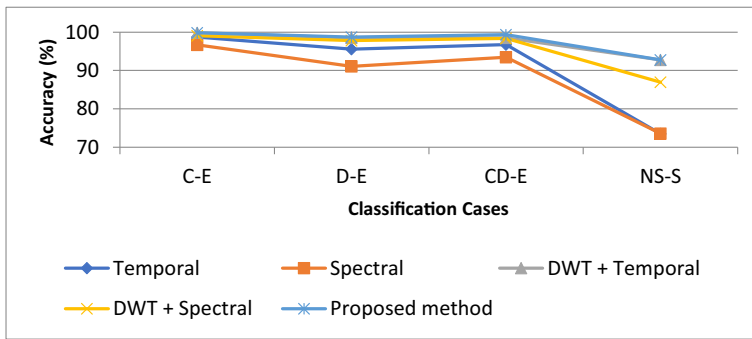


Fig. 15 Comparison of different feature vectors for EEG classification

97.15% as compared to LSTM that achieved 97.22%. For CD-E case of Bonn dataset LSTM proved the best with maximal accuracy of 99.26% however DNN and 1D-CNN obtained comparatively low score of 98.89% and 96.39% respectively. Similarly, in NS-S classification case of CHB-MIT dataset LSTM achieved the highest accuracy of 88.76% while the best specificity of 90.83% provided by DNN.

As far as the performance of hypergraph learning classifiers is concerned, HyperGCN achieved superior results as compared to HGNN for all classification cases. By using HyperGCN, the best scores as 96.63% accuracy with 96% sensitivity, 0.967 precision, and 0.595 mcc obtained in C-E classification case, however, the best specificity of 97.92% was resulted while performing CD-E classification case of Bonn dataset. In case of HGNN classifier, the C-E classification case resulted in highest accuracy of 95.45% with 94.11% sensitivity and 96.8% specificity. For NS-S classification case of CHB-MIT dataset, the obtained accuracy score was 80.29% along with 78.76% sensitivity and 81.82% specificity using HGNN while by employing HyperGCN the performance increased by 1.37% accuracy, 0.78% sensitivity and 1.96% specificity respectively.

5.6 Comparison with state-of-the-art literature works

The comparative analysis of the proposed method with previous state-of-the-art methodologies is conducted in this section. Table 17 demonstrates the comparison and depicts the superiority of the proposed method as compared to prior literature works.

Table 15 Performance comparison of the proposed feature vector with existing EEG features

Classification case	Accuracy (%)				
	Approximate Entropy	Hurst Exponent	Fractal Dimension	LBP features	Proposed feature vector
C-E	83.89	66.48	91.67	86.3	99.44
D-E	77.78	63.52	86.3	85.56	96.85
CD-E	80.37	72.84	90.25	89.01	98.64
NS-S	68.63	65.05	76.74	72.93	91.81

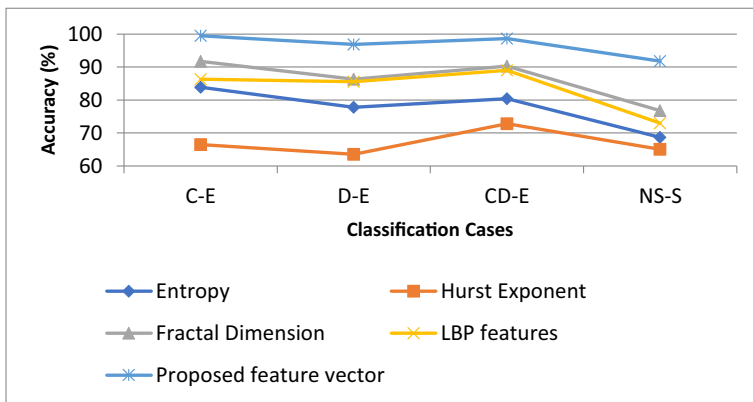


Fig. 16 Comparison of the proposed feature vector with other existing EEG features

In the case of the Bonn dataset, [4, 13, 22, 23, 37] provided percentage accuracy of 99%, 98.5%, 99%, 99.54%, and 99.5% respectively for a C-E classification case that improved to 99.81% by the proposed method. For the D-E classification case, [4, 13, 23, 30, 44] achieved accuracy percentages of 98.5%, 96%, 98.1%, 98%, and 97.5% respectively, but the proposed method enhanced the performance to 98.70%. Similarly, in the CD-E case, [4, 13, 22, 23, 29] obtained 98.67%, 97.75%, 98.5%, 98.61%, and 99% accuracies, but the proposed method boosted the classification accuracy to 99.38%.

On the other hand, using the CHB-MIT dataset, the proposed method showed an improved classification accuracy of 92.79% as compared to [28, 40], which provided 90% and 85.6% accurate classification of EEG signals for the NS-S classification case respectively.

Table 16 Performance comparison of deep learning and hypergraph learning classifiers

Dataset	Classification case	Classifier	Accuracy (%)	Sensitivity (%)	Specificity (%)	Precision	MCC
Bonn Dataset	C-E	DNN	99.81	99.62	100	0.998	0.996
		1D-CNN	98.22	97.68	98.79	0.988	0.964
		LSTM	98.89	97.73	100	0.989	0.978
		HyperGCN	96.63	96	97.26	0.967	0.959
		HGNN	95.45	94.11	96.8	0.955	0.933
	D-E	DNN	97.96	96.97	98.91	0.980	0.959
		1D-CNN	97.15	96.54	97.76	0.978	0.943
		LSTM	97.22	96.97	97.46	0.972	0.944
		HyperGCN	95.87	95.20	96.54	0.958	0.922
		HGNN	94.32	93.28	95.36	0.946	0.912
	CD-E	DNN	98.89	98.48	99.08	0.989	0.975
		1D-CNN	96.39	89.88	99.59	0.991	0.919
		LSTM	99.26	99.24	99.27	0.993	0.983
		HyperGCN	94.85	91.78	97.92	0.949	0.904
		HGNN	93.03	91.54	94.52	0.938	0.897
CHB-MIT Dataset	NS-S	DNN	88.49	86.20	90.83	0.886	0.771
		1D-CNN	83.84	81.92	85.76	0.838	0.769
		LSTM	88.76	87.62	89.91	0.888	0.775
		HyperGCN	81.66	79.54	83.78	0.816	0.678
		HGNN	80.29	78.76	81.82	0.805	0.654

Table 17 Comparative analysis of the proposed method with state-of-the-art works

[Ref.]	Dataset	Technique used	Classifier	Classification case	Accuracy (%)
[23]	Bonn dataset	DWT + Temporal, spectral, non-linear features	RF	C-E D-E CD-E CD-E	99 98.5 98.67 97.75
[29]	Bonn dataset	TQWT + Non-linear features	LS-SVM	D-E	96
[30]	Bonn dataset	EMD + Temporal, spectral features	DT	D-E	98.1
[44]	Bonn dataset	LMD + Temporal, spectral, non-linear features	GA-SVM	C-E	98.5
[37]	Bonn dataset	–	3 P-ID-CNN	C-E	99
[4]	Bonn dataset	ECT + MGT + NPT + FD + GLCM	RF	C-E D-E CD-E	98 98.5 99.54
[22]	Bonn dataset	MEMD + Temporal, Non-linear features	SVM	C-E CD-E	98.61
[13]	Bonn dataset	FBSE + WMRPE	LS-SVM	C-E D-E CD-E	99.5 97.5 99
[40]	CHB-MIT dataset	LDWT + Temporal features	SELM	NS-S	90
[28]	CHB-MIT dataset	–	DCNN	NS-S	85.6
Proposed Model	Bonn dataset	DWT + Temporal, spectral features	FRNN	C-E D-E CD-E	99.81 98.70 99.38
Proposed Model	CHB-MIT dataset	DWT + Temporal, spectral features	FRNN	NS-S	92.79

6 Conclusion

Epileptic seizures cause the dysfunction of the normal physical as well as mental health of epileptic patients. The detection of epileptic seizures using machine learning-based approaches for EEG signal classification has been frequently employed in the literature. This paper presented an improved automatic model to diagnose epileptic seizures in a clinical setup and alert medical staff about seizure occurrences in an ambulance. In this work, first, the appropriate EEG epoch size was empirically investigated for better signal interpretation. Second, a feature extraction method was proposed that inspected the most discriminating features of EEG signals to perform an effective classification. Third, fuzzy and traditional machine learning algorithms were employed for the classification of EEG epochs into interictal and ictal classes. Finally, a performance comparison of classifiers was conducted in terms of accuracy, sensitivity, specificity, precision, and MCC measures. In order to evaluate the proposed framework, two benchmark datasets, the single channel intracranial Bonn dataset and the multi-channel extracranial CHB-MIT dataset, were utilized. It was observed that KNN and FRNN achieved remarkable and convincing results for all classification cases on both datasets. As compared to the scalp EEG from the CHB-MIT dataset, intracranial EEG recordings from the Bonn dataset provided improved scores in all performance measures for classification between interictal and ictal classes. Furthermore, a comparative analysis with the existing literature proved the effectiveness of the proposed method for automatic epileptic seizure detection.

Authors contribution Aaeysa: Conceptualization, Writing – original draft, review & editing. M. Bilal Qureshi: Supervision, Review & editing. M. Afzaal: Data curation, validation, Software. M. Shuaib Qureshi: Formal analysis. M. Fayaz: Writing – review & editing, Validation.

Declarations

Competing interests The authors declare that there is no conflict of interest among authors.

References

1. Andrzejak RG, Lehnertz K, Mormann F, Rieke C, David P, Elger CE (2001) Indications of nonlinear deterministic and finite-dimensional structures in time series of brain electrical activity: dependence on recording region and brain state. *Phys Rev E* 64:061907
2. Anugraha A, Vinotha E, Anusha R, Giridhar S, Narasimhan K (2017) A machine learning application for epileptic seizure detection. *ICCIDS 2017: IEEE International Conference on Computational Intelligence in Data Science*, Chennai, pp 1–4
3. Arunkumar N, Ramkumar K, Venkatraman V, Abdulhay E, Fernandes SL, Kadry S et al (2017) Classification of focal and non focal EEG using entropies. *Pattern Recogn Lett* 94:112–117
4. Atal DK, Singh M (2019) A hybrid feature extraction and machine learning approaches for epileptic seizure detection. *Multidim Syst Sign Process*:1–23
5. Bhattacharyya A, Pachori RB (2017) A multivariate approach for patient-specific EEG seizure detection using empirical wavelet transform. *IEEE Trans Biomed Eng* 64:2003–2015
6. Bongioni L, Balbinot A (2020) Evaluation of recurrent neural networks as epileptic seizure predictor. *Array*, 100038.
7. Boughorbel S, Jarray F, El-Anbari M (2017) Optimal classifier for imbalanced data using Matthews correlation coefficient metric. *PLoS One* 12:e0177678
8. Breiman L (2001) Random forests. *Mach Learn* 45:5–32

9. Derrac J, Garcia S, Herrera F (2014) Fuzzy nearest neighbor algorithms: taxonomy, experimental analysis and prospects. *Inform Sciences* 260:98–119
10. Feng Y, You H, Zhang Z, Ji R, Gao Y (2019) Hypergraph neural networks. *Proc AAAI Conf Artificial Intell* 33:3558–3565
11. Goldberger, A. L.; Amaral, L. A.; Glass, L; Hausdorff, J. M.; Ivanov, P. C.; Mark, R. G.; et al. PhysioBank, PhysioToolkit, and PhysioNet: components of a new research resource for complex physiologic signals. *Circulation* 2000, 101, e215–e220.
12. Gu Y, Cleeren E, Dan J, Claes K, Van Paesschen W, Van Huffel S et al (2018) Comparison between scalp EEG and behind-the-ear EEG for development of a wearable seizure detection system for patients with focal epilepsy. *Sensors* 18:29–46
13. Gupta V, Pachori RB (2019) Epileptic seizure identification using entropy of FBSE based EEG rhythms. *Biomed Signal Process Control* 53:101569
14. Han J; Pei J; Kamber M (2012) *Data mining: concepts and techniques*, 3rd ed.; Elsevier
15. Hühn J, Hüllermeier E (2009) FURIA: an algorithm for unordered fuzzy rule induction. *Data Min Knowl Discov* 19:293–319
16. Jana GC, Sharma R, Agrawal A (2020) A 1D-CNN-spectrogram based approach for seizure detection from EEG signal. *Procedia Comput Sci* 167:403–412
17. Jensen R, Cornelis C (2011) Fuzzy-rough nearest neighbour classification and prediction. *Theor Comput Sci* 412:5871–5884
18. Kaburlasos VG, Athanasiadis IN, Mitkas PA (2007) Fuzzy lattice reasoning (FLR) classifier and its application for ambient ozone estimation. *Int J Approx Reason* 45:152–188
19. Khan MA, Rubab S, Kashif A, Sharif MI, Muhammad N, Shah JH, Zhang YD, Satapathy SC (2020) Lungs cancer classification from CT images: an integrated design of contrast based classical features fusion and selection. *Pattern Recogn Lett* 129:77–85
20. Li M, Chen W, Zhang T (2017) Classification of epilepsy EEG signals using DWT-based envelope analysis and neural network ensemble. *Biomed Signal Process Control* 31:357–365
21. Li M, Chen W, Zhang T (2017) Automatic epileptic EEG detection using DT-CWT-based non-linear features. *Biomed Signal Process Control* 34:114–125
22. Mahjoub C, Jeannès RLB, Lajnef T, Kachouri A (2020) Epileptic seizure detection on EEG signals using machine learning techniques and advanced preprocessing methods. *Biomed Eng/Biomedizinische Technik* 65:33–50
23. Mursalin M, Zhang Y, Chen Y, Chawla NV (2017) Automated epileptic seizure detection using improved correlation-based feature selection with random forest classifier. *Neurocomputing* 241:204–214
24. Naz I, Muhammad N, Yasmin M, Sharif M, Shah JH, Fernandes SL (2019) Robust discrimination of leukocytes protuberant types for early diagnosis of leukemia. *J Mech Med Biol* 19:1950055
25. Olokodana I, Mohanty S; Kougianos E (2020) Distributed Kriging-Bootstrapped DNN Model for Fast, Accurate Seizure Detection from EEG Signals. In *ISVLSI 2020: IEEE Computer Society Annual Symposium on VLSI*, pp. 264–269
26. Orhan U, Hekim M, Ozer M (2011) Signals classification using the K-means clustering and a multilayer perceptron neural network model. *Expert Syst Appl* 38:13475–13481
27. Orosco L, Correa AG, Diez P, Laciár E (2016) Patient non-specific algorithm for seizures detection in scalp EEG. *Comput Biol Med* 71:128–134
28. Park C, Choi G, Kim J, Kim S, Kim TJ, Min K, Jung KY, Chong J (2018) Epileptic seizure detection for multi-channel EEG with deep convolutional neural network. In *ICEIC 2018: IEEE International Conference on Electronics, Information, and Communication*, pp. 1–5
29. Patidar S, Panigrahi T (2017) Detection of epileptic seizure using Kraskov entropy applied on tunable-Q wavelet transform of EEG signals. *Biomed Signal Process Control* 34:74–80
30. Riaz F, Hassan A, Rehman S, Niazi IK, Dremstrup K (2016) EMD-based temporal and spectral features for the classification of EEG signals using supervised learning. *IEEE Trans Neural Syst Rehabil Eng* 24:28–35
31. Sarkar M (2007) Fuzzy-rough nearest neighbor algorithms in classification. *Fuzzy Sets Syst* 158:2134–2152
32. Sharif M, Amin J, Nisar MW, Anjum MA, Muhammad N, Shad SA (2020) A unified patch based method for brain tumor detection using features fusion. *Cogn Syst Res* 59:273–286
33. Shukla KK, Tiwari AK (2013) *Efficient algorithms for discrete wavelet transform: with applications to denoising and fuzzy inference systems*, Springer Science & Business Media
34. Subasi A, Kevric J, Canbaz MA (2019) Epileptic seizure detection using hybrid machine learning methods. *Neural Comput Appl* 31:317–325
35. Subramanian R, Wache J, Abadi MK, Vieriu RL, Winkler S, Sebe N (2018) ASCERTAIN: emotion and personality recognition using commercial sensors. *IEEE Trans Affect Comput* 9:147–160
36. Tiwari AK, Pachori RB, Kanhangad V, Panigrahi BK (2017) Automated diagnosis of epilepsy using key-point-based local binary pattern of EEG signals. *IEEE J Biomed Health Inform* 21:888–896

37. Ullah I, Hussain M, Aboalsamh H (2018) An automated system for epilepsy detection using EEG brain signals based on deep learning approach. *Expert Syst Appl* 107:61–71
38. Vapnik V (2013) *The nature of statistical learning theory*, Springer science & business media
39. Vidyaratne LS, Iftikharuddin KM (2017) Real-time epileptic seizure detection using EEG. *IEEE Trans Neural Syst Rehabil Eng* 25:2146–2156
40. Wang Y, Li Z, Feng L, Zheng C, Zhang W (2017) Automatic detection of epilepsy and seizure using multiclass sparse extreme learning machine classification. *Comput Math Methods Med* 2017:6849360
41. Wang X, Gong G, Li N (2019) Automated recognition of epileptic EEG states using a combination of symlet wavelet processing, gradient boosting machine, and grid search optimizer. *Sensors* 19:219
42. Yadati N, Nimishakavi M, Yadav P, Nitin V, Louis A, Talukdar P (2019) Hypergrcn: A new method for training graph convolutional networks on hypergraphs. *Advances in Neural Information Processing Systems*, pp. 1511–1522
43. Yuan Q, Zhou W, Zhang L, Zhang F, Xu F, Leng Y (2017) Epileptic seizure detection based on imbalanced classification and wavelet packet transform. *Seizure* 50:99–108
44. Zhang T, Chen W (2017) LMD based features for the automatic seizure detection of EEG signals using SVM. *IEEE Trans Neural Syst Rehabil Eng* 25:1100–1108
45. Zhang Y, Yang S, Liu Y, Zhang Y, Han B, Zhou F (2018) Integration of 24 feature types to accurately detect and predict seizures using scalp EEG signals. *Sensors* 18:1372
46. Zhao S, Gholaminejad A, Ding G, Gao Y, Han J, Keutzer K (2019) Personalized emotion recognition by personality-aware high-order learning of physiological signals. *ACM Trans Multimed Comput Commun Appl (TOMM)* 15:1–18

Publisher's note Springer Nature remains neutral with regard to jurisdictional claims in published maps and institutional affiliations.

Affiliations

**Aayesha¹ • Muhammad Bilal Qureshi¹ • Muhammad Afzaal² •
Muhammad Shuaib Qureshi³ • Muhammad Fayaz³**

Aayesha
a2z.aayesha@gmail.com

Muhammad Afzaal
muhammad.afzaal@dsv.su.se

Muhammad Shuaib Qureshi
qureshi.shuaib@gmail.com

Muhammad Fayaz

¹ muhammad.fayaz@ucentralasia.org
Department of Computer Science, Shaheed Zulfikar Ali Bhutto Institute of Science and Technology, Islamabad 44000, Pakistan

² Department of Computer and Systems Sciences, Stockholm University, Stockholm, Sweden

³ Department of Computer Science, School of Arts and Sciences, University of Central Asia, Bishkek, Kyrgyz Republic